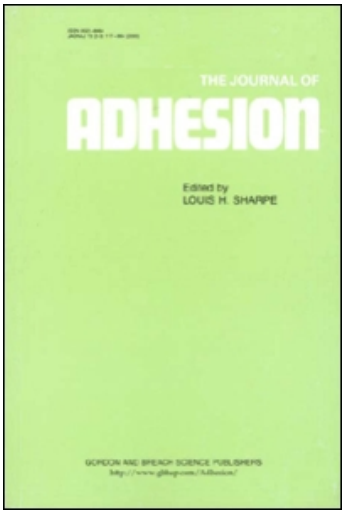

The Journal of Adhesion
Publication details, including instructions for authors and subscription information:
http://www.informaworld.com/smpp/title~content=t713453635

Molecular Dynamic Simulation of Adhesional Release of Particles from Surfaces

D. J. Quesnel[a]; D. S. Rimai[b]; L. P. Demejo[b]
[a] Mechanical Engineering Department, University of Rochester, Rochester, NY, USA [b] Office Imaging Research and Technology Development, Eastman Kodak Company, Rochester, NY, USA

To cite this Article Quesnel, D. J. , Rimai, D. S. and Demejo, L. P.(1998) 'Molecular Dynamic Simulation of Adhesional Release of Particles from Surfaces', The Journal of Adhesion, 67: 1, 235 — 257
To link to this Article: DOI: 10.1080/00218469808011110
URL: http://dx.doi.org/10.1080/00218469808011110

J. Adhesion, 1998, Vol. 67, pp. 235–257
Reprints available directly from the publisher
Photocopying permitted by license only

Molecular Dynamic Simulation of Adhesional Release of Particles from Surfaces*

D. J. QUESNEL [a], D. S. RIMAI [b,**] and L. P. DEMEJO [b]

[a]*Mechanical Engineering Department, University of Rochester, Rochester, NY 14627-0132, USA;*
[b]*Office Imaging Research and Technology Development, Eastman Kodak Company, Rochester, NY 14653-6402, USA*

(Received 19 May 1997; In final form 11 October 1997)

The generalized form of the Lennard-Jones soft-sphere pair potential is used to examine the adhesional attachment and release behavior of particles on surfaces for materials of varying "ductility". Using a two-dimensional simulation, with the repulsive term held constant at $m = 12$, the attractive term is varied from $n = 2$ to $n = 10$ at a constant binding energy to provide a controlled way of changing the effective range of interaction between atoms. Molecular dynamics simulates the placement of particles on a free surface and the subsequent removal of these particles by controlling the displacement of the center of mass. Simulations indicate that the longer-ranged removal forces literally tear out a chunk of the surface by pulling out a tether-like strand connecting the ball and plate. As the forces become shorter range, the size of the region of disturbed material after separation decreases until, at the shortest range, only three atoms are transferred and there is relatively little damage to the system on separation as indicated by the lack of slip steps in the plate. Results are discussed both mechanistically and from the point of view of more traditional approaches to surface force behavior, such as the JKR and DMT models.

Keywords: Molecular dynamics; particle adhesion; particle separation; Lennard-Jones; JKR theory; DMT theory

* Presented at the Symposium on *Fundamentals of Adhesion and Interfaces* at the Fall Meeting of the American Chemical Society in Orlando, Florida, USA, August 25–28, 1996.

** Corresponding author.

INTRODUCTION

The adhesion of particles to a surface is governed by a combination of surface energetics and mechanical response of the contacting materials. These effects have been described in numerous theories by researchers such as Derjaguin [1], Bradley [2, 3], Hamaker [4], Krupp [5] and Maugis and Pollock [6]. Dominating current particle adhesion theory are the models proposed by Johnson *et al.* [7], referred to as the JKR theory, and that of Derjaguin and coworkers [8], referred to as the DMT theory. As discussed by Tabor [9], these theories do not predict the same adhesional behavior between particles and substrates. Rather, the DMT theory predicts that the contact radius at equilibrium, under conditions of no externally applied load, would be approximately half that predicted by the JKR theory. As a result, the DMT theory predicts that the work of adhesion, for a given size contact radius, is eight times that predicted by the JKR model. Moreover, the externally-applied force needed to effect separation of the particle from the substrate predicted by the DMT theory is 4/3 that predicted by the JKR model. Finally, the JKR model predicts that separation occurs at a finite contact radius equal to approximately 0.63 of the equilibrium contact radius in the absence on an externally-applied force, whereas the DMT theory requires that the contact radius vanish prior to separation. These discrepancies were resolved by the work of Muller *et al.* [10, 11] (hereafter referred to as the MYD model), who showed that they arose from differing assumptions regarding the shape of the contact zone. Moreover, the MYD model argues that the DMT theory should hold for smaller particles in systems with high elastic moduli and low surface energy, whereas the JKR theory is more suitable for larger particles and systems with higher surface energies and lower elastic moduli. The transition between these theories is given by the relation $\mu = 1$ where μ is defined by

$$\mu = \frac{32}{3\pi}\left[\frac{2R w_A^2}{\pi E^{*2} z_0^3}\right]^{1/3} \tag{1}$$

where

$$\frac{1}{E^*} = \frac{(1-\nu_1^2)}{E_1} + \frac{(1-\nu_2^2)}{E_2} \tag{2}$$

and R is the particle radius, w_A the work of adhesion, z_0 the separation distance between the particle and substrate (or, more precisely, the equilibrium separation between two adhering half-spaces), and ν_i and E_i the Poisson ratio and Young's modulus of each material, respectively.

These theories all approach the mathematical representation of particle adhesion on a macroscopic level, whereas the physics of particle adhesion occurs at the molecular level. Moreover, the same potentials that give rise to the mechanical properties of materials also give rise to those properties normally associated with adhesion, such as surface energy. When particles adhere to surfaces, local changes in the structure of the particle and surface take place. These changes depend on the detailed forces acting on each atom. The accumulated forces of all the atoms in the surface on all the atoms in the particle represent the total force of the surface on the particle and *vice versa*. Naturally, any change in material type will influence the adhesion by changing the rules under which the atoms attract one another, thereby influencing all other material properties that are macroscopically used to characterize the materials. Having investigated the mechanical properties of simple Lennard-Jones solids, their interfacial energetics, and their bonding to surfaces, the present paper addresses the issues associated with particle detachment. As in our earlier works, this paper is intended to elucidate the physics of the processes involved in the phenomena investigated rather than produce precise quantitative predictions for specific materials systems. Even so, it has been shown in the previous papers [12, 13], discussing elastic moduli, Poisson's ratio and interfacial energy, that the predictions of this modelling, when applied in three dimensions, has been very effective for quintessential Lennard-Jones materials such as argon as well as for polymeric materials, such as polyethylene and polypropylene, where the polymer chains interact *via* van der Waals forces. More recently, the use of two-dimensional modelling and the Lennard-Jones potential have served well in the studies of the basic phenomena governing the impact and adhesion of particles to surfaces [14, 15]. Although this is a more similar analogy to a cylinder, rather than a sphere, in contact with a plane, the qualitative physics of adhesion can still be studied.

Following this philosophy, the present work uses two-dimensional modelling and Lennard-Jones potentials to explore the fundamental

aspects of particle removal. Using a more generalized form of the Lennard-Jones potential [16], sometimes referred to as the Mie potential, the effective range of interaction between the atoms can be changed while holding the binding energy between the atoms constant. Enhanced ductility is exhibited by those models with longer ranges of interatomic interaction, while increased brittleness is observed when the range of interaction is reduced. This provides for a very effective tool to examine the applicability of the JKR and DMT theories from a microscopic point of view.

COMPUTATIONAL PROCEDURE

In this work, the generalized soft-sphere Lennard-Jones Potential, where the exponents in the attractive and repulsive terms are variables, is used to generate force-distance relationships between the atoms that have varying ranges of attraction. This can be done at constant total binding energy by using the following form [16]:

$$\Phi(r, n, m) = k(n, m) \cdot \varepsilon \cdot \left[\left(\frac{\sigma}{r}\right)^n - \left(\frac{\sigma}{r}\right)^m\right] \tag{3}$$

where

$$k(n, m) = \frac{n}{n - m}\left(\frac{n}{m}\right)^{\left(\frac{m}{n-m}\right)} \tag{4}$$

has a value of $k(6, 12) = -4$ leading to the familiar 6–12 form of the potential with the leading -4ε term, which has been shown to represent inert gases and polymers rather well [13, 14] with respect to their elastic properties [17, 18] and surface energies [19].

In implementing the molecular dynamics code, the potential is analytically differentiated to yield the force between atoms as a function of distance. The exponent m, which controls the strength of the repulsive term was held constant at 12 while n, which controls the spatial extent of the attractive term, was varied from $n=2$ to $n=10$. This range is selected because it represents the largest range over which the calculations can give useful results. Figure 1 shows the functional form of the interatomic force law obtained by differentiation of the

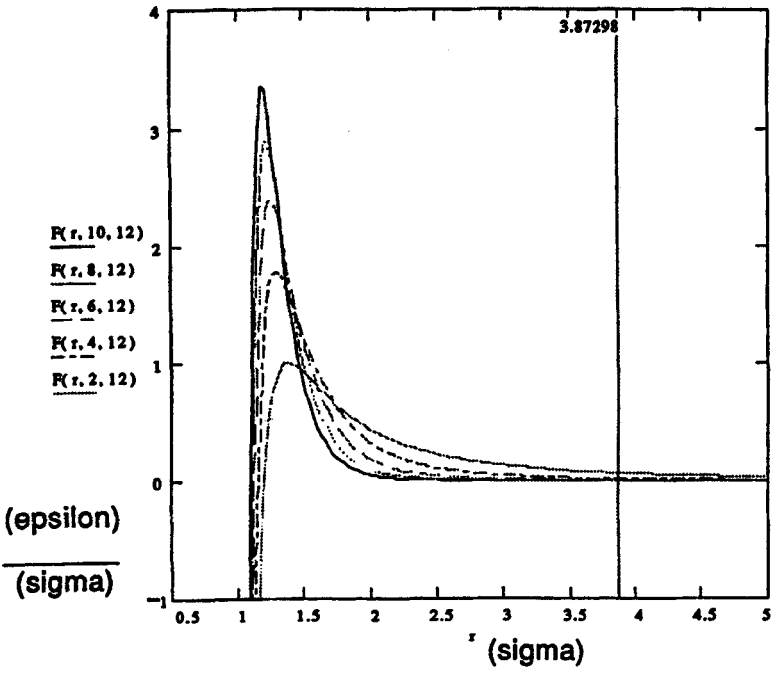

FIGURE 1 The Lennard-Jones force law for even values of the parameter n. Note the range of interactions and the equilibrium (zero force) point decreases with increasing n, while the maximum value of the force increases with increasing n. These shifts occur in such a way to maintain a constant binding energy, ε, the area under the curve between the zero force point and infinity.

potential for even values of n from 2 to 10. Note that only the $n = 2$ case is showing any significant force at 3.87298 σ, which is the value of the cutoff radius used for interatomic interactions in these computations. The integral of each of these curves from infinity to the zero crossing represents the binding energy, ε, which was held constant in the present calculations.

Changing the range of the interatomic potential at constant binding energy will alter the mass density of a stress-free system. To implement properly the force laws of differing ranges of interaction requires a detailed knowledge of the initial interatomic spacing of the stress-free state including effects attributable to thermal expansion. Otherwise, substantial internal stresses will be present in the system. Because the systems of interest contain free surfaces, these internal residual stresses

can produce large-scale plastic deformation, destabilizing the entire geometry, and overwhelming any effects associated with adhesion. To determine the proper initial spacing to produce a stress-free system, the initial pressure on the system before the atoms has time to move was computed as a function of the size scale of the initial configuration. The spacing required for zero pressure at the start of the calculation was determined to several significant figures using a manual root-finding scheme. This result, equivalent to the equilibrium spacing at the absolute zero of temperature, is shown in Figure 2 as a decreasing function of the attraction exponent, n. The equilibrium spacing varies from 1.127 to 1.0925 as n varies from 2 to 10, about a 3.5% effect. While these may seem like trivially small changes, when they are considered as strains, and with respect to the stresses needed to produce them, they are comparable with the theoretical strength of crystals and are substantially above the yield strengths of these materials.

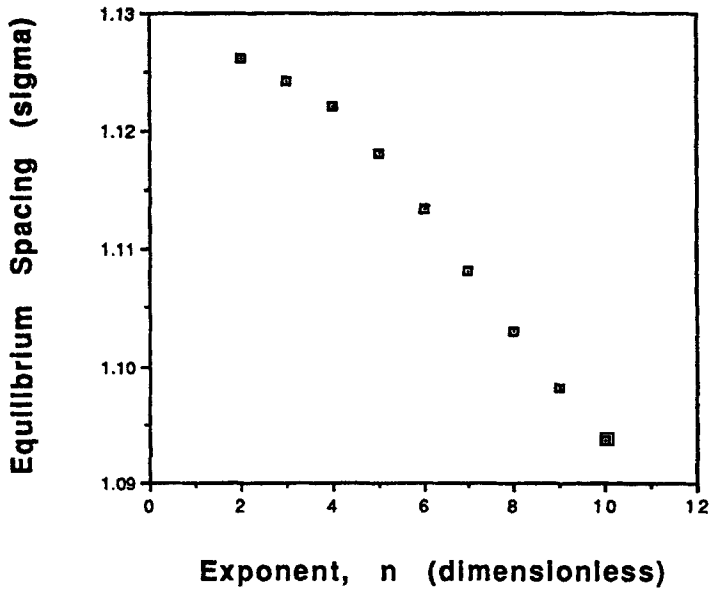

FIGURE 2 Equilibrium interatomic spacing needed for zero initial pressure during the simulation for various n at fixed $m = 12$ in the generalized soft-sphere Lennard-Jones law.

The equilibrium spacing for collections of atoms shown in Figure 2 is not the same as that for single atom pairs represented by the force equal zero point in Figure 1. Both increase as the potential becomes longer-ranged, that is, as n decreases, but not at the same rate. The general reason for the increase with longer-ranged potentials is the lower overall force of attraction required to maintain a constant binding energy. This allows the repulsive term to push the equilibrium point to larger spacings. The equilibrium spacing for collections of atoms increases less rapidly with decreasing n than for pairs of atoms because the far field attractions associated with decreased n are stronger for the longer-ranged interactions and act to compress the structure. This *action at a distance* produces an overall qualitative change in the behavior of the materials with the more long-range interactions leading to more ductile behavior and the shorter range (but higher force) demonstrating more brittle behaviors.

With the equilibrium spacing properly identified, the atoms are placed into a particle (circle) and a surface (rectangle) that each contain a hexagonal lattice. The circle and rectangle start at a separation of one cutoff radius so that the atoms at the edges of the circle and rectangle do not sense any forces from one another. The lattices of the circle and the rectangle are rotated by 30 degrees from one another to minimize any tendency for epitaxial attachment.

The computational system is allowed to evolve for 100 iterations without any modification in energy or dimensions in order to allow the system to come to equilibrium. During this time, equipartitioning of the potential and kinetic energies occurs. A data stream is established from which temperature and pressure can be computed. After the initial 100 iterations, the temperature and pressure controllers are turned on and the system is allowed to equilibrate for an additional 900 iterations. Plots of all key parameters as a function of time are now stable.

PARTICLE APPROACH AND ADHESION

The particle is then thrown towards the surface with an initial velocity. The temperature controller is running so that the initial velocity is rapidly damped since any motion of atoms is interpreted as kinetic

energy. The initial velocity is chosen so that the velocity of the particle as it reaches the surface is low enough not to cause any substantial mechanical damage. The effects of impact velocity are discussed more fully elsewhere [15]. For all intents and puposes, this is a critically damped descent onto the surface. Once the particle is in contact with the surface, an additional 1000 iterations are allowed to establish once again the system equilibrium.

During this time, the particle joined the surface with the establishment of a contact patch or neck as shown in Figure 3. Figure 3a shows the system in equilibrium for $n = 3$, representing interatomic forces with a long range of interaction. Figure 3b is the $n = 6$ case

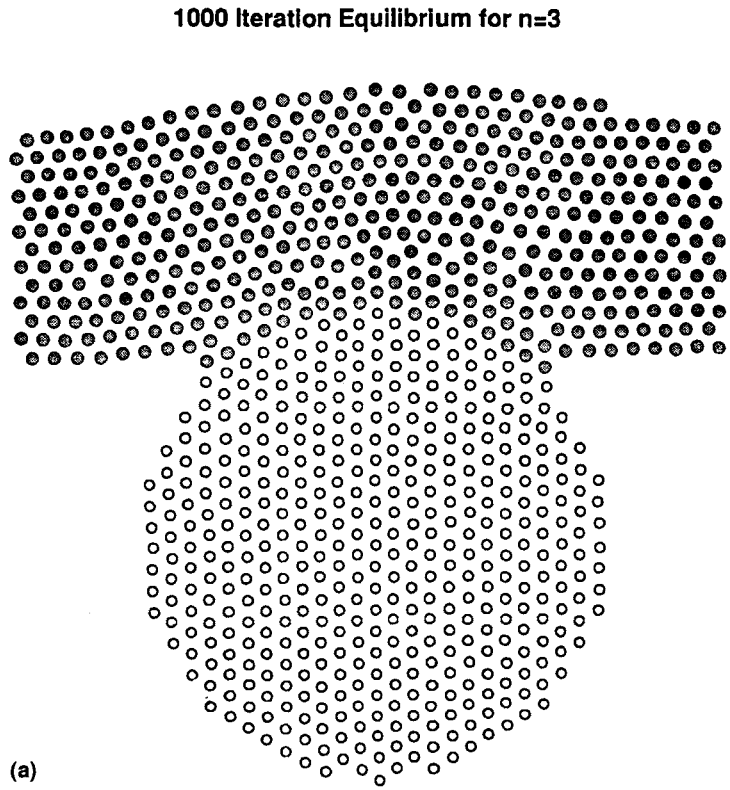

FIGURE 3 Morphology of the particle on the surface after equilibration for 1000 computational iterations. (a) for longest range forces with $n=3$, (b) for the standard Lennard-Jones system with $n=6$, and (c) for the shortest range forces with $n=9$.

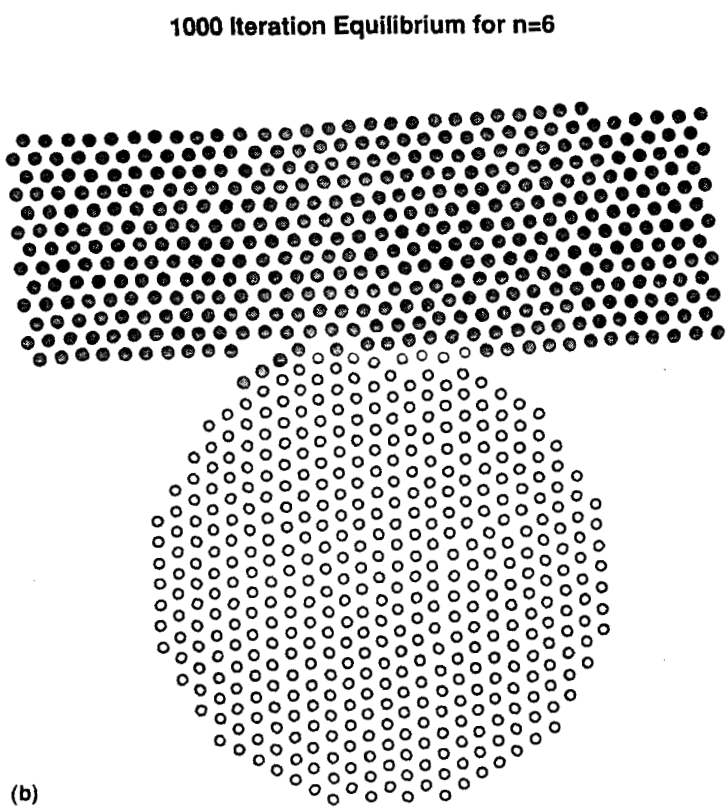

FIGURE 3 (Continued).

representing the usual Lennard-Jones force law. Figure 3c is for short range forces characterized by $n = 9$. Note that the dimensions of the zero applied force contact patch increase as the forces become more long-range and decrease as the forces become more short-range. The atoms of the long-range force case seem to epitax to the particle, producing a grain boundary type defect well within the surface, complete with dislocation generation, as the particle is actually pulled into the surface by the interatomic surface by the interatomic forces. In the long-range case, Figure 3c, only a few point defects are created and there is very little deformation of the materials caused by the surface forces. The grain boundary representing the orientation mismatch

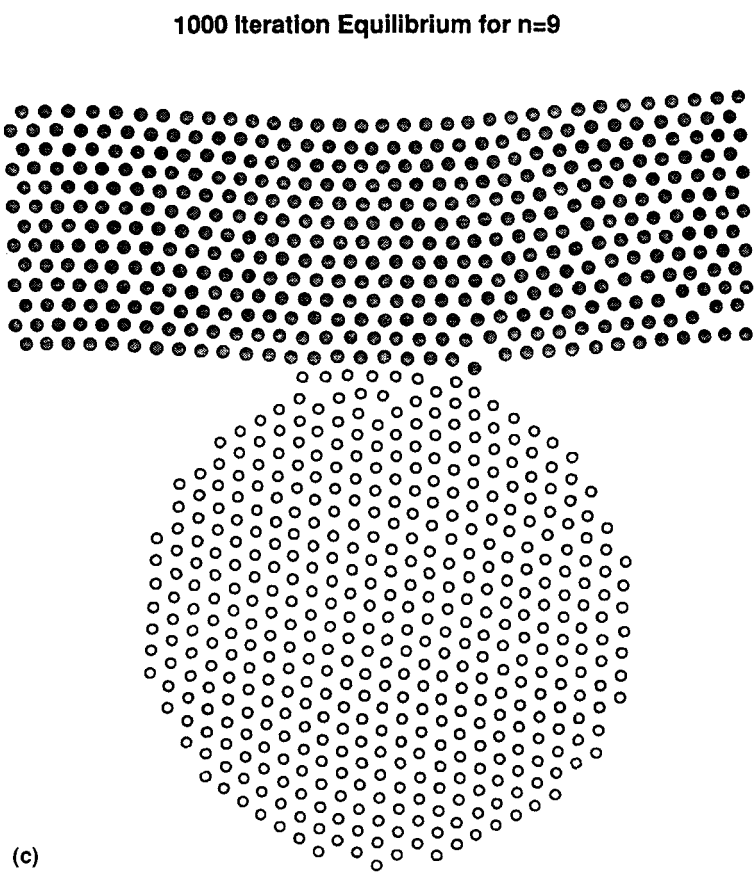

FIGURE 3 (Continued).

remains sharply defined at the original surface. These observations demonstrate clearly that the surface forces that arise naturally from interatomic forces in these molecular dynamic simulations are capable of inducing deformation in the materials with the degree of deformation dependent on the range of interaction of the force law. Similar physical observations have been made by Rimai *et al.* [20, 21] in the case of PDMS substrates with polyurethane spheres.

Figure 4 summarizes the equilibrium neck width for all of the values of n. Recall that large n means short-ranged, yet larger, forces between atoms while smaller n implies longer-ranged, yet smaller magnitude,

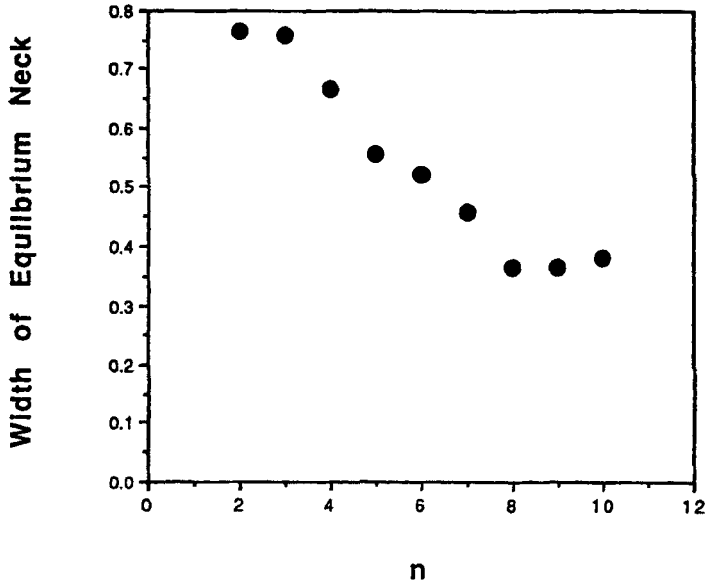

FIGURE 4 Equilibrium width of the neck that forms between the particle and the surface for various values of the parameter n. Note the larger n, responsible for the shorter range forces, produce a smaller neck. Neck width is dimensionless, expressed in terms of the unstrained diameter of the particle.

forces. The exponent, n, is dimensionless while the equilibrium neck width is expressed in units of the diameter of the particle (circle). The equilibrium neck width changes by about a factor of two as n varies from 3 to 8. Naturally, if we think of this phenomenon as surface force or surface energy driven, we would conclude that the larger neck width is the result of a larger surface energy and that the larger surface energy is causing deformations of the system. Since the only thing changed in this simulation is the range of the interaction, it seems rational to conclude that surface energy is not localizable to the surface for such small systems. Rather, it is the manifestation of all of the attractions between all the atoms in one particle for all the atoms in the other. The true surface portion is only the effect attributable to first nearest neighbors and with weaker, longer-range force law, this should imply smaller surface forces but in fact, the weaker, longer-range force law, acting over much larger distances dominates the behavior causing an apparently larger effect. Surface energies are not

just first nearest neighbor phenomena, but rather reflect all of the broken bonding in systems where second, third, etc., bonds are involved. Changing the overall strength of the bond will also affect the numerical value of the surface energy, but this effect also modifies the elastic properties.

These phenomena combine to suggest that the surface energy and surface forces we often discuss have two sources, the strength of the interatomic bonding and the range over which these bonds act. The range of interaction appears to dominate the effects we see in this molecular dynamic modelling where the strength of the bond, that is the binding energy between atoms, has been held constant. It is likely that this is an even more significant effect in three dimensions where contributions from neighbors in the third direction could also contribute to the interatomic forces.

ADHESIONAL RELEASE

The particle is now removed from the surface by moving the center of mass of those atoms initially in the circle (particle) away from the center of mass of those atoms initially in the rectangle (surface). This is accomplished during 1000 steps leading to a net separation of one cutoff radius, essentially generating the starting condition if on interactions had occurred. During the removal process, the system is allowed to evolve and remain at equilibrium. The adhesional release process begins when the neck extends and thins under the applied deformation. This thinning is accompanied by dislocation and point defect generation. At some point, the neck fractures and it is interesting to note that the fracture does not occur at a particular size for all cases but rather depends on the range of the potential.

Figures 5a, 5b and 5c show the microstructure of the particle and substrate after separation of the centroids by one cutoff radius. Figure 5a is associated with the long range ($n = 3$) force law and the neck does not actually fracture. Rather, the substrate appears to form a neck connecting the particle and substrate. There is epitaxy between the particle and the neck with what appears to be a tearing of a substantial portion of the substrate leaving a scar in the substrate similar to what occurs during wear associated with adhesive processes.

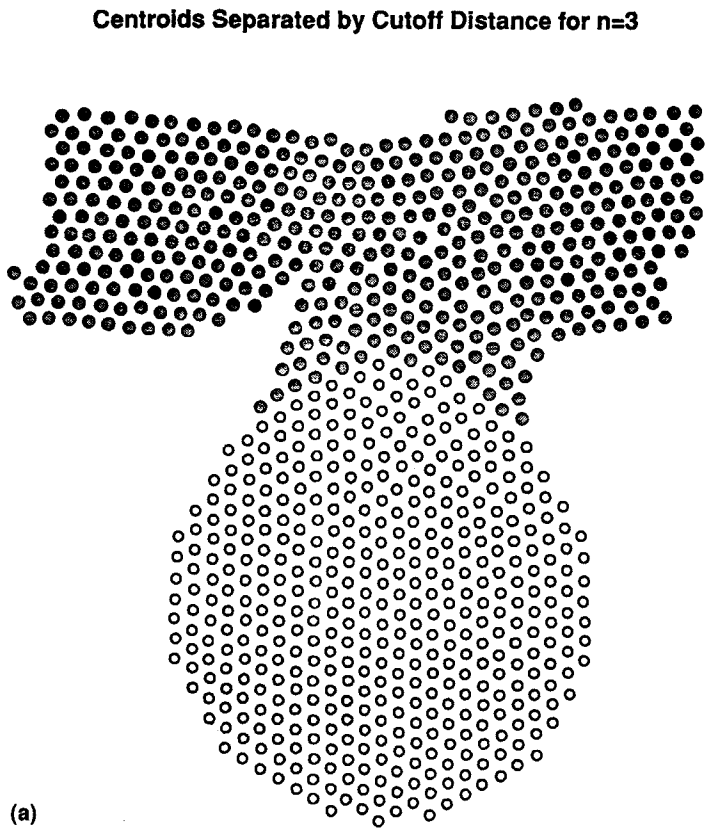

FIGURE 5 Morphology of the particle substrate system after the centroids have been separated by one cut off radius. (a) indicates a tether left behind with cracks into the substrate, (b) indicates a fracture with material transfer, and (c) shows reduced defect production and material transfer as the range of interactions of the interatomic potential are decreased.

Figure 5b represents the behavior characteristic of van der Waals interactions ($n = 6$). Here approximately 20 atoms are transferred from the substrate to the particle. Moreover, an atom of the particle remains on the surface adjacent to a vacancy formed in the substrate. Evidence of dislocation motion is present in the form of slip steps on the back surface of the substrate. The location of the fracture surface is consistent with cohesional failure within the bulk of one of the contacting materials rather than adhesional failure at the interface

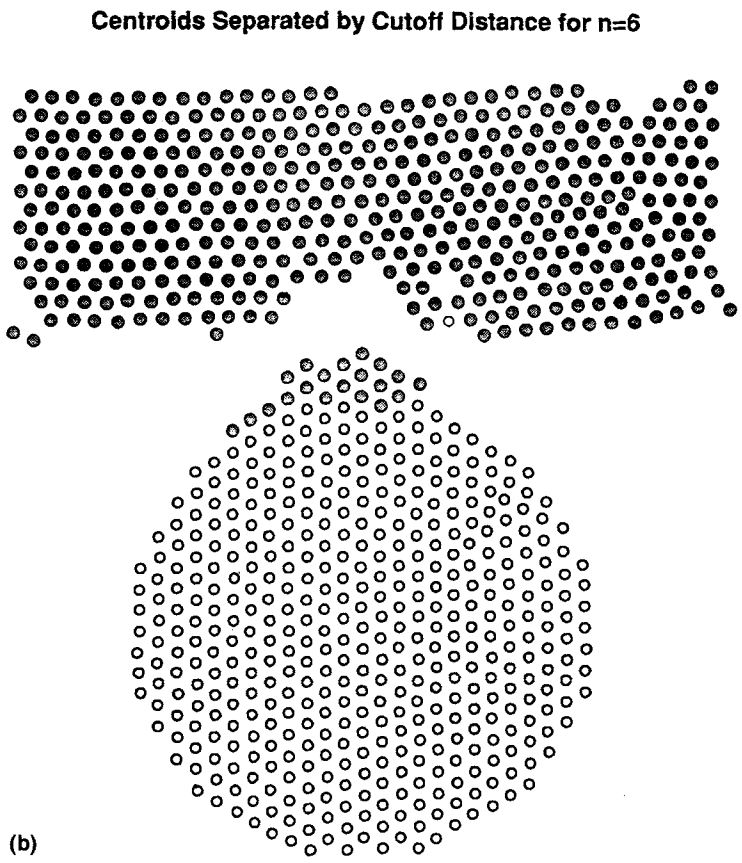

FIGURE 5 (Continued).

[22, 23]. The separation is observed to occur from a finite contact radius rather than when the contact radius vanishes. Finally, Figure 5c documents the situation for the short-range interactions where the exponent in the potential, n, equals 9. Here, only eight atoms are transferred and these are from the particle to the substrate leaving a small hillock on the surface. Virtually no deformation has occurred in either the substrate or the particle with the fracture surfaces exhibiting geometries suggesting a perfect match when fitted back together, typical of fracture surfaces observed for brittle materials.

Since it is clear that there is a systematic change in the fracture size scale with the range of the potential, it is useful to examine this in more

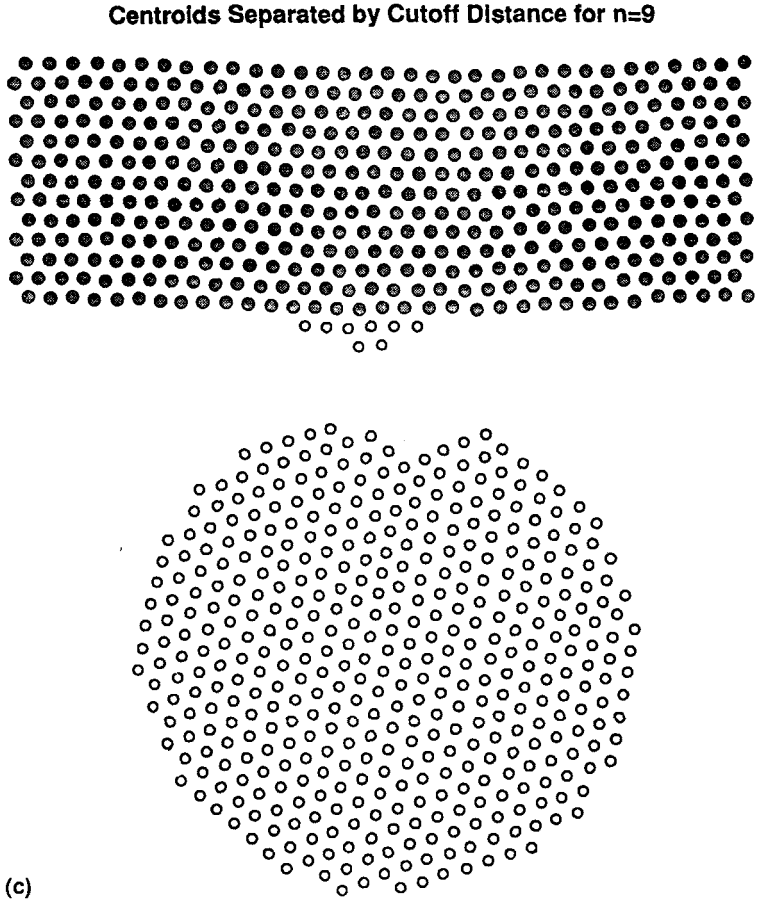

FIGURE 5 (Continued).

detail. Figures 6a and 6b illustrate the sizes of the fracture. Figure 6a shows the neck size at rupture in units of the diameter of the particle. There is a monotonic increase in the size of the neck at rupture as the range of the force law increases, that is, an n increases. For the n equal 2 and 3 cases, rupture did not occur and the neck extended and maintained a diameter of approximately 0.60 – 0.65 of the particle diameter.

Figure 6b complements the results in Figure 6a by showing the width of the fracture scar observable after separation, again in units of

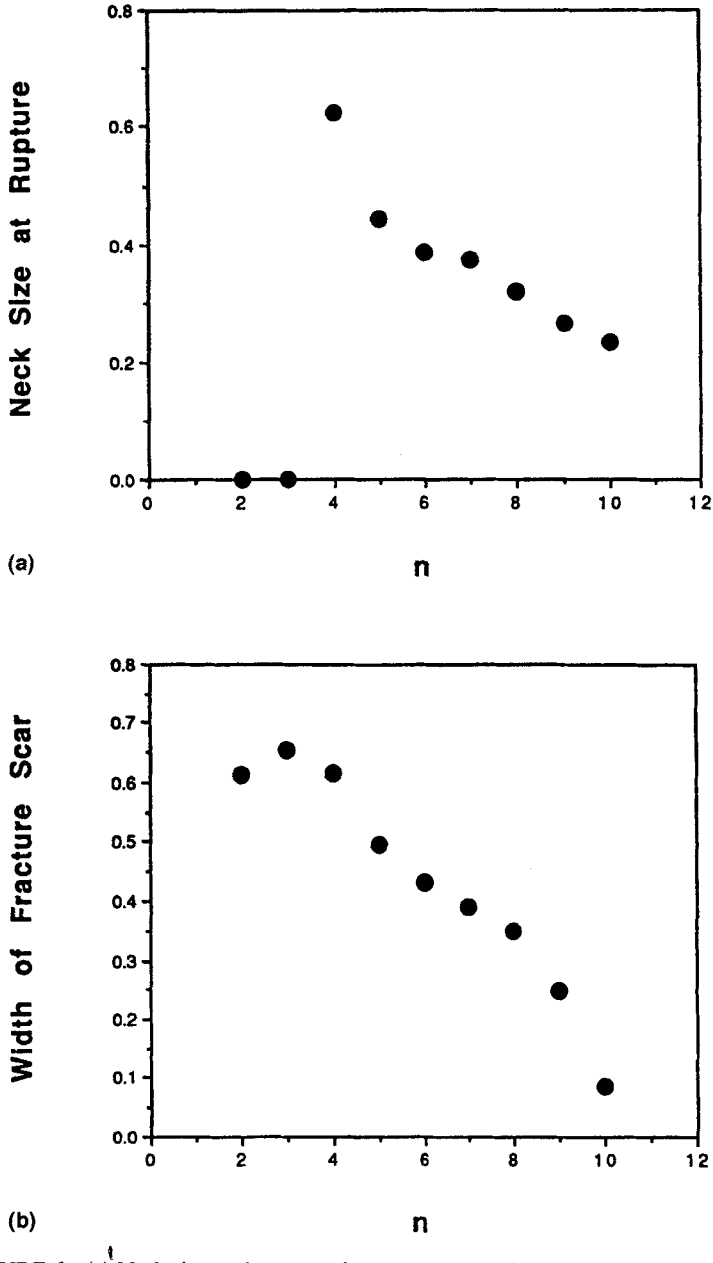

FIGURE 6 (a) Neck size at the onset of rupture expressed in terms of the unstrained diameter of the particle. For $n = 2$ and $n = 3$, a tether was formed. Where fracture did occur, a smooth decrease in neck size with range of interaction as characterized by the parameter n is shown. (b) Width of the fracture scar left behind, a second measure of the size of the neck at fracture.

the diameter of the particle. The remaining ligament width is plotted for the low n cases that did not show separation. A smooth curve is formed with the fracture scar widths of those with shorter ranges of interaction and, hence, larger n. The very small fracture scar for the largest n is the result of the surface rehealing rather well. During the adhesional release, the neck narrowed to a string of single atoms that fractured leaving only two atoms on the surface.

Figure 7 shows the forces generated between the particle and the surface during removal. It is computed by determining the total normal force exerted by all the atoms in the surface on all the atoms in the particle at each step of the removal process. These data are plotted, curve fitted, and the maximum value is extracted from the curve. The force of removal appears to be relatively insensitive to the range of the force law with the higher individual forces counterbalanced by fewer short range for all but the largest n. A slight upward trend may be indicative of DMT-like behavior as the range of the potential decreases. This is considered more fully in the discussion section.

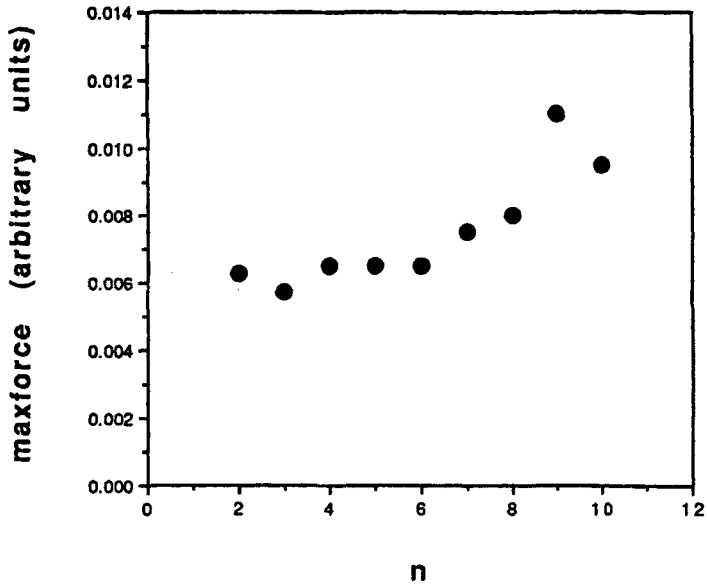

FIGURE 7 Maximum force needed to remove the particles as a function of the parameter n characterizing the range of interatomic interactions. The larger removal forces are for the shorter ranged interactions where individual forces were higher.

DISCUSSION

Particle adhesion theory today is dominated principally by two models. The first, proposed by Johnson, Kendall, and Roberts, (hereafter referred to as JKR) assumed that all interactions occur within the actual contact radius. According to this model, the contact radius a is related to the particle radius R, the applied load P, and the thermodynamic work of adhesion w_A by

$$a^3 = \frac{R}{K}\{P + 3w_A\pi RP + [6w_A\pi RP + (3w_A\pi R)^2]^{1/2}\} \quad (5)$$

K is related to the Poisson ratios ν_i and Young's moduli E_i by the equation

$$K = \frac{4}{3\pi(k_1 + k_2)} \quad (6)$$

where k_i are given by

$$k_i = \frac{1 - \nu_i^2}{\pi E_i} \quad (7)$$

If there is no applied load, Equation (5) reduces to

$$a_0^3 = \frac{6w_A\pi R^2}{K} \quad (8)$$

Alternatively, if a negative load is applied, the contact radius decreases. However, the requirement that the solutions to Equation (5) be real limits the decrease in the contact radius. Specifically, at an applied load of

$$P_s = -\frac{3}{2}w_A\pi R \quad (9)$$

corresponding to a contact radius a_s, equal to approximately 0.63 a_0, separation of the particle from the substrate occurs. It is a characteristic of the JKR model that particle-substrate separation occurs at a finite contact radius rather than when a vanishes.

An alternative description of particle adhesion was proposed by Derjaguin *et al.* (hereafter referred to as DMT) [8]. This model assumes that the contact radius is Hertzian. As a result of this assumption, the force of attraction equipartitions, with exactly half occurring within the contact radius and half occurring outside. As shown by Tabor [9], the differing assumptions in the two models lead to different predictions of adhesional behavior. Specifically, the contact radius predicted by the DMT model is approximately half that predicted by the JKR formalism. Moreover, the DMT model predicts that separation occurs when the contact radius vanishes. Finally, the force needed to effect separation according to the DMT model is 4/3 of that predicted by JKR.

A resolution of these discrepancies was proposed by Muller *et al.* (hereafter referred to as MYD) [10, 11] who showed that the JKR model and the DMT model were applicable in different regions of the contact zone; the regions of applicability being defined by the parameter μ given in Equation (1). The DMT to JKR transition was discussed by Maugis and Gauthier-Manuel [24]. In general, the JKR theory would be the appropriate choice for describing the adhesion of particles having diameters greater than approximately 1 μm. DMT theory might be appropriate to describe aerosol particles. JKR behavior has been experimentally verified [20]. No conclusive experimental verification of the DMT theory exists at this time.

Although these theories describe particle adhesion in a practical sense, they are not holistic. Specifically, the aforementioned theories assume that the existence of parameters such as the Young's modulus and Poisson's ratio are independent of other factors affecting adhesion, such as the surface energies. This has led to a phenomenological approach to particle adhesion behavior. For example, the instability discussed earlier in this paper with respect to Equation (5) is given as the reason why the JKR theory predicts separation at a finite radius, since the solution becomes imaginary for greater negative applied loads. However, the JKR theory does not address the physics of the separation process. In fact, one could question how an elastic theory, such as the JKR theory, would adequately predict separation behavior, when the fracture occurring during separation is clearly inelastic.

Moreover, the JKR and DMT models each make specific assumptions about the shape of the contact, resulting in vastly

different predictions of the adhesional behavior, as discussed by Tabor. Even the MYD model, which attempts to unify these theories, assumes that the mechanical response of the materials is independent of the surface energetics. The MYD model further assumes that the interactions between the two bodies can be determined by a simple pairwise summation of the interactions between the atoms in the two materials, without allowing the atoms to move in response to the forces.

An alternative approach to understanding particle adhesion, at least qualitatively, has been reported by Quesnel *et al.* [12–15]. According to this model, the mechanical properties and surface energetics are both related to the same interatomic potential, making the adhesional behavior a consequence of how the atoms interact. Although it is recognized that this model has been explored using relatively small particles and two-dimensional calculations, it still sheds light on the underlying physics of particle adhesion. Moreover, it is extendable to larger and three-dimensional particles and substrates by using supercomputers and/or parallel processing.

Results from the present computations can be used to determine the physics behind the adhesional observations and predictions of the JKR and DMT models. As presented earlier, it is clear that the range of the interaction of the potential and, hence, the range of interaction of the force law, provides a change in the size of the contact area at fracture during the application of a negative force to the particle. In particular, the longest range interactions lead to the largest contact areas as shown in Figures 6a and 6b. The equilibrium neck size is also shown to decrease with decreasing range of the potential as shown in Figure 4.

Because the JKR and DMT models make predictions in terms of the ratio of the contact radius at failure to the equilibrium contact radius, it is appropriate to plot the computational results in this form, as shown in Figure 8. The ratio of rupture size to the contact radius at equilibrium is observed to be in the neighborhood of 0.7 to 0.8 and appears to decrease slowly with decreasing range of the potential (higher n). This seems to be in reasonable agreement with the 0.63 prediction of the JKR model for the three-dimensional case, but inconsistent with the DMT prediction that the contact radius continually decreases to zero at separation. It is interesting to note that the particles used in these compuations would correspond to nanoclusters. Furthermore, these results are independent of Young's

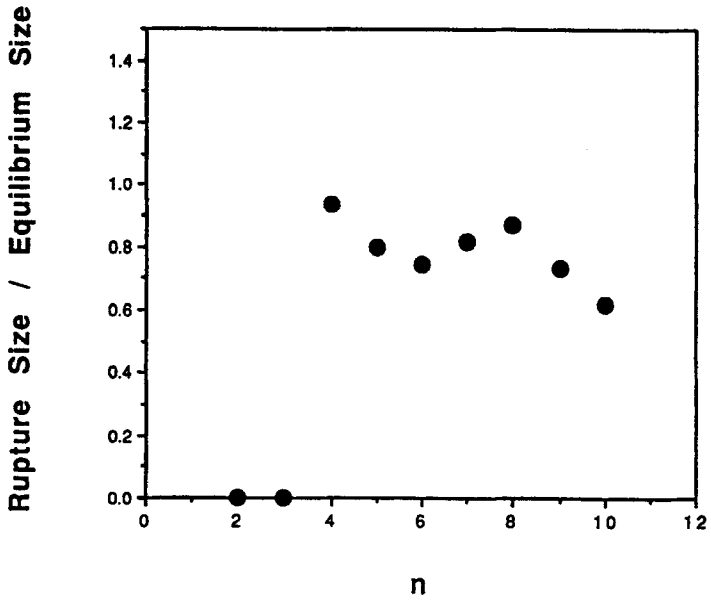

FIGURE 8 Ratio of the rupture diameter of the neck to the equilibrium diameter of the contact with zero applied load. This ratio is useful for comparison with three dimensional predictions of the JKR and DMT models. No information is presented for the $n = 2$ and $n = 3$ cases where a tether was formed.

Modulus since both sigma and epsilon of Equation (1) have not been specified.

As previously discussed, the computed force of separation (see Fig. 7) appears to increase slowly with decreasing range of potential. Coupled with the slowly decreasing dependence of the ratio a_s/a_0 on n, this result suggests that the DMT theory may hold for very short-range potentials rather than for small particles. Perhaps this is consistent with the MYD prediction that the DMT model would hold for higher modulus materials. Indeed, there is a gradual stiffening (suggesting higher modulus) with increasing n, as shown in Figure 1, to support this conjecture.

SUMMARY

The behavior of two-dimensional particles and surfaces has been studied using molecular dyanmics to model particle attachment and

forced removal from surfaces. In this work, the focus was on systematically varying the range of interaction of the atoms by varying the exponent n, which controls the attractive force term in the generalized soft-sphere Lennard-Jones force law. It was found that long-range force laws (low n) favor fracture at a finite and large-sized contact radius, comparable with the contact size at zero force, while short-range force laws favor necking down to very small sizes before fracture occurs. At $n = 6$, where model parameters represent polymers well, the computation shows contact radii at fracture to be 0.7 of the zero-load contact radii, independent of Young's modulus. These results suggest that the JKR model may be appropriate to describe particle adhesion even on the nanometer-size scale. Finally, the results of these calculations suggest that particle-substrate separation is accompanied by a cohesional failure in the bulk of at least one of the materials rather than simple adhesional failure at the interface.

References

[1] Derjaguin, B. V., *Kolloid Z.* **69**, 155 (1934).
[2] Bradley, R. S., *Philos. Mag.* **13**, 853 (1932).
[3] Bradley, R. S., *Trans. Faraday Soc.* **32**, 1088 (1936).
[4] Hamaker, H. C., *Physics* **4**, 1058 (1937).
[5] Krupp, H., *Adv. Colloid Interface Sci.* **1**, 111 (1967).
[6] Maugis, D. and Pollock, H. M., *Acta Metall.* **32**, 1323 (1984).
[7] Johnson, K. L., Kendall, K. and Roberts, A. D., *Proc. R. Soc. London Ser.* **A324**, 301 (1971).
[8] Derjaguin, B. V., Muller, V. M. and Toporov, P. Yu., *J. Colloid Interface Sci.* **53**, 314 (1975).
[9] Tabor, D., *J. Colloid Interface Sci.* **58**, 2 (1977).
[10] Muller, V. M., Yushchenko, V. S. and Derjaguin, B. V., *J. Colloid Interface Sci.* **77**, 97 (1980).
[11] Muller, V. M., Derjaguin, B. V. and Toporov, Yu. P., *Colloids Surf.* **7**, 251 (1983).
[12] Quesnel, D. J., Rimai, D. S. and DeMejo, L. P., *Solid State Commun.* **85**, 171 (1993).
[13] Quesnel, D. J., Rimai, D. S. and DeMejo, L. P., *Phys. Rev. B*, **48**, 6795 (1993).
[14] Quesnel, D. J., Rimai, D. S. and DeMejo, L. P., *J. Adhesion Sci. Technol.* **9**, 1015 (1995). See also Quesnel, D. J., Rimai, D. S. and DeMejo, L. P., in *Fundamentals of Adhesion and Interfaces*, Rimai, D. S., DeMejo, L. P. and Mittal, K. L., Eds. (VSP, Utrecht, 1995) pp. 281–296.
[15] Quesnel, D. J., Rimai, D. S. and DeMejo, L. P., *J. Adhesion* **51**, 49 (1995). See also Quesnel, D. J., Rimai, D. S. and DeMejo, L. P., in *Advances in Particle Adhesion*, Rimai, D. S. and Sharpe L. H., Eds. (Gorden and Breach, Amsterdam, 1996) pp. 49–69.
[16] Haile, J. M., *Molecular-Dynamics Simulation: Elementary Methods* (Wiley, New York, 1992).

[17] Simmons, G. and Wang, H., *Single-Crystal Elastic Constants and Calculated Aggregrate Properties:* A Handbook, 2nd edition (MIT Press, Cambridge, 1971).
[18] Van Krevelen, D. W., *Properties of Polymers* (Elsevier, Amsterdam, 1976).
[19] Wu, S., *Polymer Interfaces and Adhesion* (Dekker, New York, 1982).
[20] DeMejo, L. P., Rimai, D. S., Chen, J. H. and Bowen, R., in *Particles on Surfaces: Detection, Adhesion and Removal*, Mittal, K. L., Ed. (Marcel Dekker, New York, 1995); see also Rimai, D. S., DeMejo, L. P. and Bowen, R. C., *J. Adhesion Sci. Technol.* **8**, 1333 (1994).
[21] DeMejo, L. P., Rimai, D. S., Chen, J. H. and Bowen, R. C., *J. Adhesion* **48**, 47 (1995).
[22] Sharpe, L. H., *J. Adhesion* (to be published).
[23] Bikerman, S. J., *The Science of Adhesion Joints* (Academic Press, New York 1968) pp. 137.
[24] Maugis, D. and Gauthier-Manuel, B., in *Fundamentals of Adhesion and Interfaces*, Rimai, D. S., DeMejo, L. P. and Mittal K. L., Ed. (VSP, Utrecht, 1995) pp. 49–60.
[25] DeMejo, L. P., Rimai, D. S. and Bowen, R. C., *J. Adhesion Sci. Technol.* **5**, 959 (1991).